Integrated Dissemination System of Frequency, Time and Data for Radio Astronomy

Link to publication record in Manchester Research Explorer

OPEN ACCESS

Integrated Dissemination System of Frequency, Time and Data for Radio Astronomy

Yufeng Chen
Bo Wang
Lijun Wang
Keith Grainge
Richard Oberland
Richard Whitaker
Althea Wilkinson
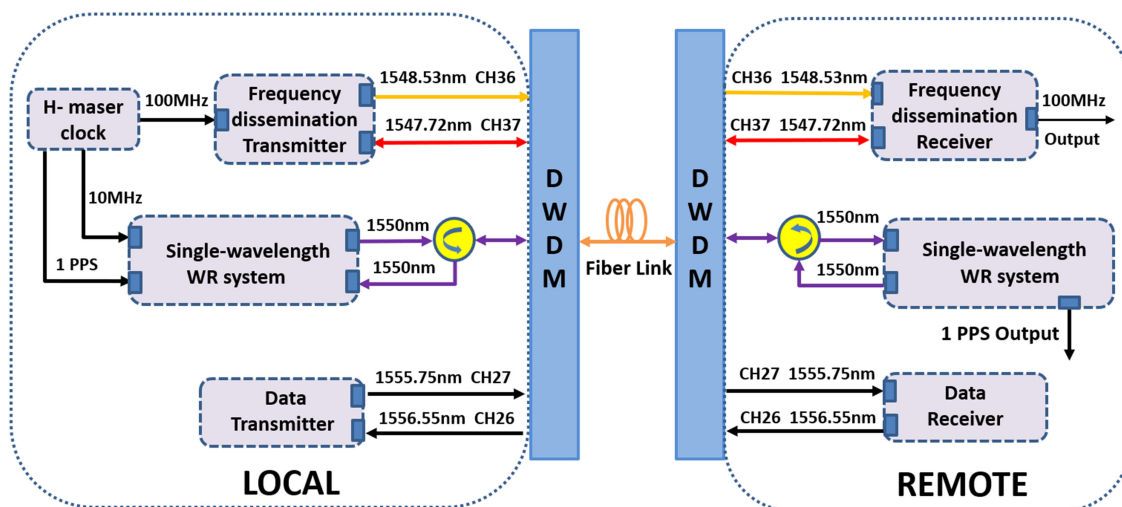
Integrated Dissemination System of Frequency, Time and Data for Radio Astronomy

Yufeng Chen,[1,2] **Bo Wang,**[1,2] **Lijun Wang,**[1,2] **Keith Grainge,**[3]
Richard Oberland,[3] **Richard Whitaker,**[3] **and Althea Wilkinson**[3]

[1]State Key Laboratory of Precision Measurement Technology and Instruments, Department
of Precision Instrument, Tsinghua University, Beijing 100084, China
[2]Key Laboratory of Photonic Control Technology (Tsinghua University), Ministry of
Education, Beijing 100084, China
[3]Jodrell Bank Centre for Astrophysics, Alan Turing Building, School of Physics &
Astronomy, The University of Manchester, Manchester M13 9PL, U.K.

Abstract: For radio telescope array applications, the precise time and frequency reference predominantly determines the quality of the observation. In this paper, we demonstrate an integrated dissemination system which can achieve ultra-stable frequency dissemination, time synchronization and data transfer simultaneously over a single optical fiber link. The test of this integrated system was carried out on the 48-km fiber link, which consisted of 28-km buried fibers, and 20-km fiber spool in laboratory. It has been experimentally demonstrated that the frequency transfer stability is $2.6 \times 10^{-14}/s$ and $3.0 \times 10^{-16}/10^4 s$. The time synchronization with 100-ps accuracy and the error bit ratio of data transfer at the level of 10^{-8} are also demonstrated.

Index Terms: Integrated dissemination system, frequency dissemination, time synchronization, data transfer.

1. Introduction

In the field of radio astronomy, such as the Very Long Baseline Interferometry (VLBI) [1], to implement the interferometry observation, each antenna needs precise and stable time and frequency (T&F) reference, which is used to sample the received antenna signals [2], [3]. Then, these digitized antenna data are transferred to the correlator for finally acquiring the values of fringe visibility function. However, signals received by individual antenna are not correlated during the observation, which will result in relatively large loss of coherence. To ensure the mutual coherence of the signals recorded at all stations, the receivers and the data formatters need to be synchronized to a common time and frequency reference [2]. Active Hydrogen masers (H-masers), owning to their excellent short-term stability, are usually chosen as the local frequency and time reference [4], [5].

With the development of fiber-based synchronization technology, disseminating the time and frequency reference of H-maser clock with high precision becomes feasible [6]–[9]. Using this
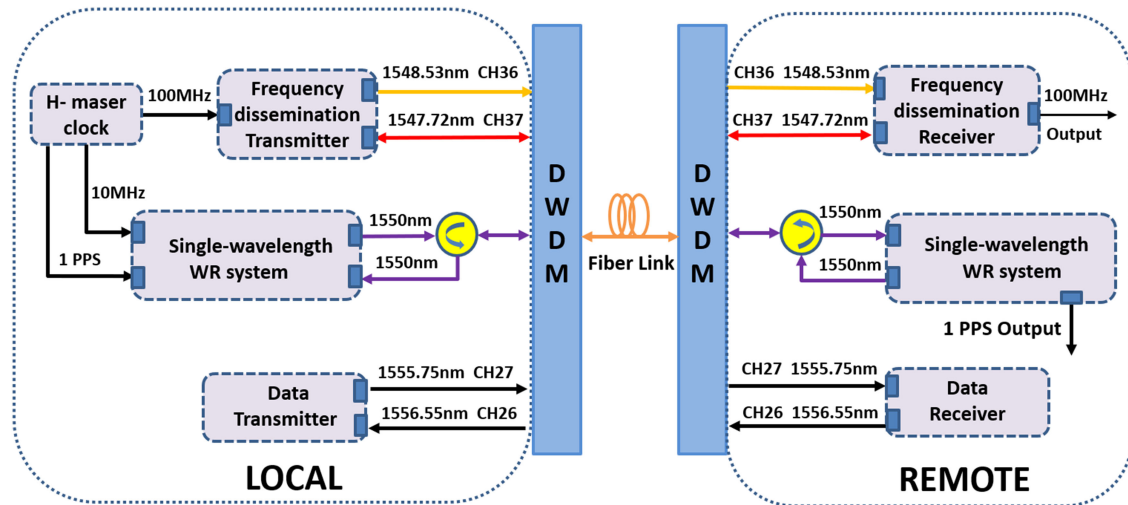
Fig. 1. Schematic diagram of the integrated dissemination system. Two custom-designed DWDM devices are used to integrate frequency dissemination part, time synchronization part and data transmission part into a whole system.

technology, the H-maser signal at the central station can be recovered at other stations to achieve the interferometry observation with good coherence. The antenna data can be transferred to the correlator through the optical fiber due to its high-speed data transmission capability. However, to the best of our knowledge, in radio telescope array applications, such as Square Kilometer Array (SKA) and e-Merlin [10]–[12], time synchronization system, frequency dissemination system and data transfer system are separate in general, and at least three fiber links are needed.

In this paper, an integrated dissemination system is demonstrated, and the dense wavelength-division multiplexing (DWDM) technology is applied [13]. With this technology, different wavelengths of light can be fed into the same fiber. Therefore, it can save a lot of fiber resources and make the system simpler when used for simultaneous time and frequency synchronization and data transfer. There are two custom-designed DWDM devices in the integrated system, with one in the transmitter for putting different wavelengths of lights together and the other in the receiver for separating them. The field test was implemented in Jodrell Bank Observatory and the frequency transfer stability is $2.6 \times 10^{-14}/s$, and $3.0 \times 10^{-16}/10^4 s$. The results of time synchronization with 100-ps accuracy, and the bit error ratio (BER) of data transfer before forward error correction (FEC) at the level of 10^{-8} are also demonstrated.

2. Experiment Setup

Fig. 1 shows the schematic diagram of the integrated dissemination system. This system can be divided into three parts, namely frequency dissemination part, time synchronization part and data transmission part. These three parts are combined with two custom-designed DWDM devices. For the frequency dissemination part, the 1f-2f dissemination method proposed in [6] is used to achieve the frequency dissemination. The main idea of this method is that the phase fluctuation of 2-GHz signal accumulated over one-way fiber link is equal to the phase fluctuation of 1-GHz signal accumulated over round-trip fiber link. The bandwidth of the phase-locked loop (PLL) at RX side is 10 Hz. To make the frequency dissemination part suitable to the DWDM devices, the wavelengths of the commercial EA-DFB lasers on the local site and the remote site are chosen as 1548.53 nm and 1547.72 nm, respectively.

For the time synchronization part, the White Rabbit (WR) technology is chosen as the solution [14], [15]. Generally, the wavelengths of laser in master and slave of WR system are different. As

a result, the effect of chromatic dispersion cannot be ignored and the fiber asymmetry needs to be calibrated to eliminate this effect [15]. The fiber asymmetry is defined by the following (1):

$$\alpha = \frac{\delta_{ms}}{\delta_{sm}} - 1 = \frac{n_{\lambda_m}}{n_{\lambda_s}} - 1 \tag{1}$$

Here, α is the fiber asymmetry, and δ_{ms} and δ_{sm} are the fiber propagation delays from master to slave and from slave to master, respectively. n_{λ_m} and n_{λ_s} are the refractive indexes for the wavelength of the lasers in the transmitter and receiver, respectively. The process of the fiber asymmetry calibration is relatively complex [16]. When the fiber link changes, for example, a new fiber is added, the fiber asymmetry coefficient needs to be calibrated again, since the refractive indexes may vary slightly when the fiber is produced by a different company or it is a different batch of fiber produced by the same manufacturer. To avoid such complex process and largely reduce the effect of chromatic dispersion, the single wavelength method proposed in [17] is used and the common wavelength of 1550 nm is selected. With two circulators are used at TX side and RX side, respectively, the optical signal from both sides can transmit in the same fiber. The isolations of the two circulators are both ~40 dBm, thus the effect of back reflection can be largely reduced. Therefore, we just need to calibrate the bitslide values and the transmission and reception delays of master and slave to minimize the asymmetry of link delay. The bitslide value is the time delay when aligning the recovered clock signal to the inter-symbol boundaries of the data stream, and can be read directly from the WR software when other delays are initially set to 0 [16]. The transmission and reception delays of master and slave can be calibrated using a pair of WR calibrators with known transmission and reception delays. To achieve the dissemination of the 1-PPS (one Pulse Per Second) signal, the WR system on the local site is referenced by the 1-PPS signal and 10-MHz signal of H-maser.

As for the data transfer part, we use the optical networking equipment (model FSP 3000R7, ADVA Corporation) to explore the mutual influence between high-speed data transmission and time-frequency dissemination. The data provided by the ADVA FSP 3000R7 equipment is 100G Ethernet, and the actual bit rate is 120.58 Gbits/s accounting for all of the overheads. The modulation format was coherent 100G DP-QPSK (dual polarization quadrature phase shift keying). This equipment is connected to the integrated system through fiber link, and the wavelengths this equipment uses are 1555.75 nm and 1556.55 nm in the transmitter and receiver, respectively. To evaluate the performance of this part, the bit error ratio (BER) before forward error correction (FEC) is calculated by this equipment. As a tool to reconstruct missing or corrupted data, FEC techniques have been adopted as a standard technique by the International Telecommunication Union — Telecommunication Standardization Sector (ITU-T) G.975 for improving the performance of digital optical communication networks at low cost [18].

Fig. 2 presents the schematic diagram of the experimental setup over 48-km fiber link, which consists of 28-km buried fiber from Jodrell Bank Observatory to Pickmere dish and 20-km fiber spool at Jodrell Bank Observatory. The 28-km buried fiber is part of the e-Merlin Array Telescopes, and the 20-km fiber spool is placed in laboratory. The 100-MHz signal generated by the H-maser clock placed at the Jodrell Bank Observatory is split into two signals. One is used as the reference of phase noise measurement device (model 5125A, Microsemi Corporation), and the other is the input of the integrated system. The 10-MHz signal and 1-PPS signal from H-maser clock serve as the reference of the WR system. The 1-PPS signal from H-maser is split into two signals, one for the reference of WR master and the other for the Start input of time interval counter (model 53230A, Keysight Technologies Corporation). The Stop input of time interval counter is the 1-PPS output of WR slave. As for the data transfer setup, the transmitter and receiver are placed in the same room in Jodrell Bank Observatory. The relevant parameters of the data transfer, such as the power of laser and the BER, can be obtained in real time from the monitoring computer.

The optical powers of frequency signals are 1.5 dBm and 1.1 dBm (for 1547.72 nm and 1548.53 nm, respectively) at TX side and −12.7 dBm and −13.8 dBm at RX side. The optical power of WR signal (1550 nm) is 1.7 dBm at TX side and −14.4 dBm at RX side (from TX side to RX side). The optical power of data signal (1555.75 nm) is 1.0 dBm at TX side and −14.1 dBm at RX side.
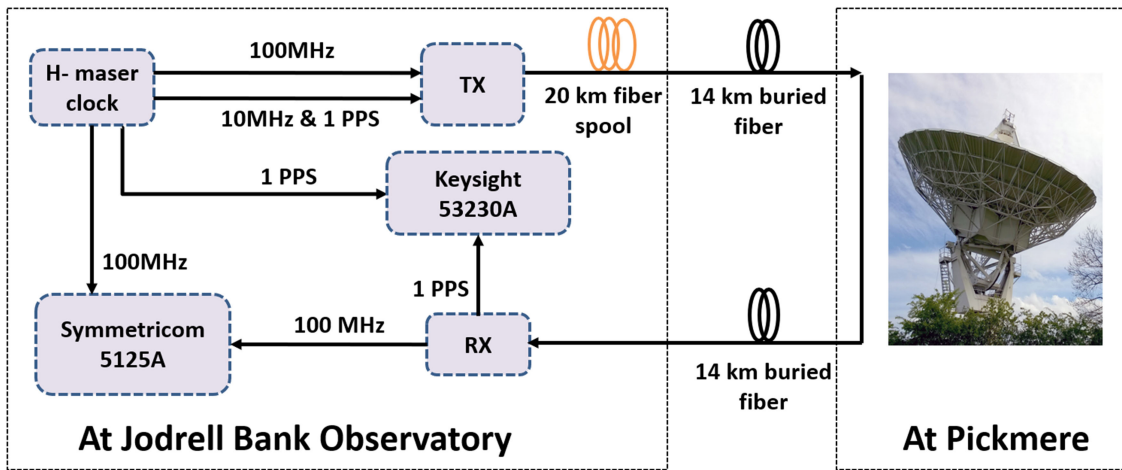
Fig. 2. Schematic diagram of the experimental setup.
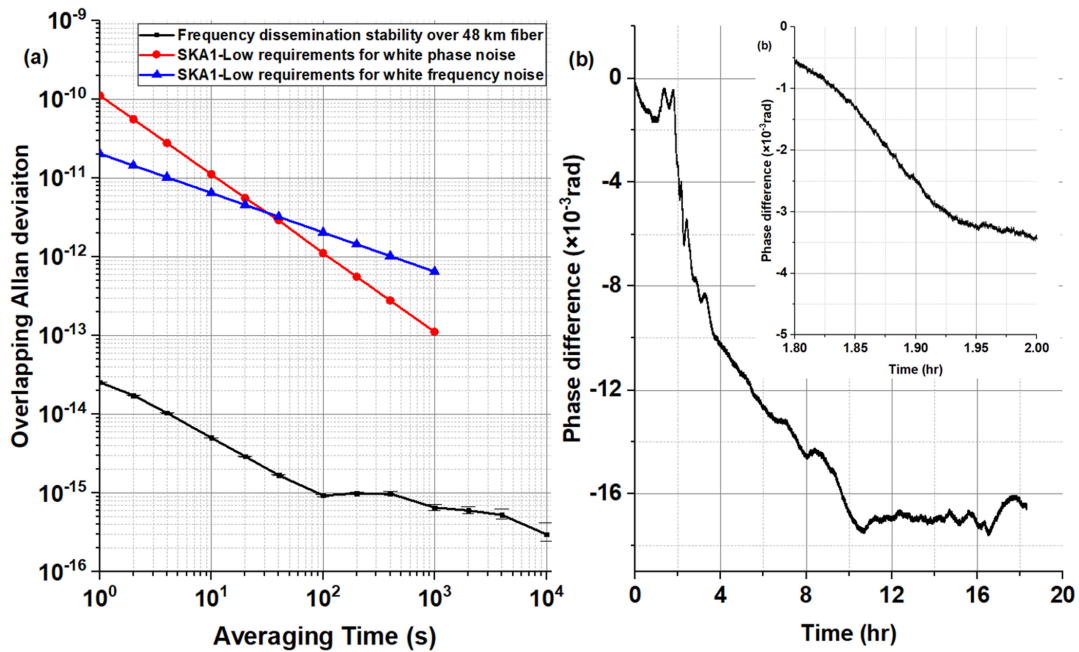
Fig. 3. (a) Overlapping Allan deviation of frequency dissemination and the requirements of SKA1-Low for white phase noise and white frequency noise in terms of Allan deviation. (b) The phase difference of 100-MHz reference signal and recovered signal. The figure in the upper right is a larger version of the fastest phase difference change part.

The optical attenuation of the 48-km fiber link is 10.3 dB and the total optical attenuation of the two circulators is 1.5 dB. The optical attenuation of DWDM filters' each channel varies slightly. The total optical attenuation of the link including the DWDM filters and circulators is about 15 dB.

Fig. 4. (a) The time synchronization results, with the mean of -8.9 ps and the standard deviation of 28.4 ps. The red line shows the result when the adjacent-averaging algorithm with 60 points as the window is used to smooth the time deviation data. (b) The histogram and the normal distribution fitting of the time synchronization errors.

3. Results and Discussion

Fig. 3(a) shows the measured frequency stability of this fiber dissemination link. The black line is the result of overlapping Allan deviation (OADEV). The bandwidth of the phase noise measurement system (5125A) is 0.5 Hz and the frequency dissemination has a stability of $2.6 \times 10^{-14}/s$ and $3.0 \times 10^{-16}/10^4 s$. Compared to the frequency dissemination stability result over 50-km fiber in [6] where $3.7 \times 10^{-14}/s$ and $2.7 \times 10^{-16}/10^4 s$ was achieved, the high-speed data transmission in the integrated system has little effect on the frequency dissemination. As shown in Fig. 3(a), we find that the OADEV after 100 s is not ideal. We think it is caused by the out-of-loop components of the frequency dissemination system, and the finite measurement time. For comparison, we also show the requirements of the low frequency aperture array in the first phase of SKA (SKA1-Low). To realize the radio astronomy interferometry, the received signals of the radio interferometry array need to be coherent. However, any instability among the frequency references in the array will lead to coherence loss. Therefore, to limit the effect of the frequency instability, the coherence requirements of SKA1-Low are put forward that the SKA1-Low reference frequency shall provide a 2% maximum coherence loss for interval of 1 second or 1 minute and up to an operating frequency of 350 MHz [19]. The conversion formula between Allan deviation and coherence loss can be found in [20]. From the comparison in Fig. 3(a) we can clearly see that the frequency dissemination stability is much better than the requirements of SKA1-Low. Fig. 3(b) shows the phase difference between the reference signal of H-maser and the recovered signal in the receiver. We still take the requirements of SKA1-Low as an example for comparison. The SKA1-Low requires the reference frequency shall have a phase drift of less than 1 radian, over intervals of up to 10 minutes and up to an operating frequency of 350 MHz. If the frequency is converted from 350 MHz to 100 MHz which is the recovered frequency of the integrated system, the requirements of less than 1 radian will be changed to less than 0.3 radian. It can be obtained from the phase difference data that the phase drift of the integrated system is less than 0.005 rad in any 10-minute interval, which can meet the SKA1-Low requirements very well.

Fig. 4(a) shows the time synchronization error of the WR part. The black line is the original result of the time synchronization error changing over time. Almost all data points are within ± 100 ps, which shows the sub-nanosecond time synchronization has been achieved. To further analyze the performance of time synchronization, the mean of -8.9 ps and the standard deviation of 28.4 ps are obtained. The standard deviation shows the WR part can realize the time synchronization with sub-50 picoseconds precision. Compared to the standard deviation of 27 ps of time synchronization
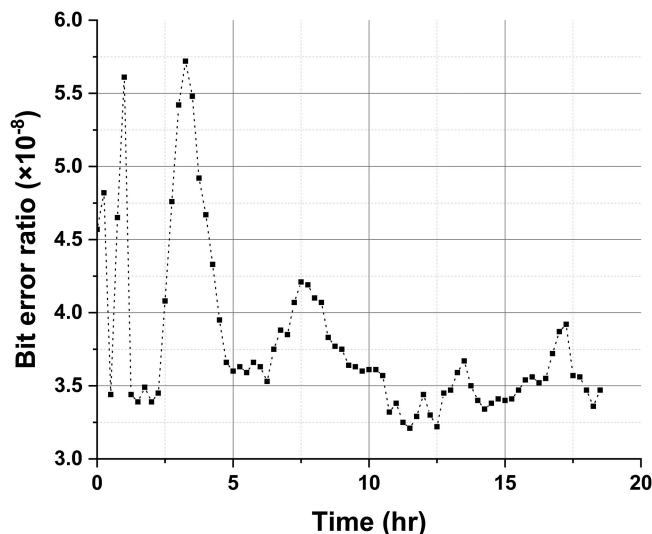
Fig. 5. The bit error ratio of the data transfer during this test at the level of 10^{-8}.

error over 50-km fiber in [17], the high-speed data transmission in the integrated system has little effect on the time synchronization. To smooth the time deviation data, the adjacent-averaging algorithm with 60 points as the window is used, and the result after smoothing is given by the red line. Fig. 4(b) shows the histogram and the normal distribution fitting of the time synchronization error. Through this figure, we can see the overall distribution of the time synchronization errors more clearly.

Fig. 5 shows the bit error ratio of the data transfer part. Although the value of the bit error ratio fluctuates to a certain extent, it is still at the level of 10^{-8} overall. According to the ITU-T Recommendation G.975.1, if the super-FEC code with three times iterative decoding is used, when the input BER is 3.1×10^{-3} the output BER will be 1.0×10^{-16} [21]. Therefore, when the BER is at the level of 10^{-8}, the output BER after FEC will be less than 1.0×10^{-16}. Such a low BER means that erroneous bits in the transmission can be ignored.

4. Conclusion

In summary, we demonstrate an integrated dissemination system of frequency, time and data for radio astronomy. With this integrated system where the DWDM technology is applied, only a single optical fiber is needed to achieve the dissemination of the above three parts. The field test was conducted in Jodrell Bank Observatory and it has been experimentally demonstrated that the frequency transfer stability is $2.6 \times 10^{-14}/s$ and $3.0 \times 10^{-16}/10^4 s$. The results of time synchronization with 100-ps accuracy, and the error bit rate of data transfer before FEC at the level of 10^{-8} are also demonstrated.

References

[1] H. Schuh and D. Behrend, "VLBI: A fascinating technique for geodesy and astrometry," *J. Geodyn.*, vol. 61, pp. 68–80, 2012.
[2] P. Krehlik *et al.*, "Fibre-optic delivery of time and frequency to VLBI station," *A & A.*, vol. 603, no. 48, 2017.
[3] Y. He *et al.*, "Long-distance telecom-fiber transfer of a radio-frequency reference for radio astronomy," *Optica*, vol. 5, no. 2, pp. 138–146, 2018.
[4] Y. Guo *et al.*, "Correlation measurement of co-located hydrogen masers," *Metrologia*, vol. 55, no. 5, pp. 631–636, 2018.
[5] M. Rioja, R. Dodson, Y. Asaki, J. Hartnett, and S. Tingay, "The impact of frequency standards on coherence in VLBI at the highest frequencies," *Astron. J.*, vol. 144, no. 4, 2012.

[6] B. Wang, X. Zhu, C. Gao, Y. Bai, J. Dong, and L. Wang, "Square kilometre array telescope-precision reference frequency synchronisation via 1f-2f dissemination," *Sci. Rep.*, vol. 5, 2015, Art. no. 13852.

[7] B. Wang *et al.*, "Precise and continuous time and frequency synchronisation at the $5 \times 10-19$ accuracy level," *Sci. Rep.*, vol. 2, pp. 556, 2012.

[8] L. Śliwczyński, P. Krehlik, and M. Lipiński, "Optical fibers in time and frequency transfer," *Meas. Sci. Technol.*, vol. 21, no. 7, 2010.

[9] F. Narbonneau *et al.*, "High resolution frequency standard dissemination via optical fiber metropolitan network," *Rev. Sci. Instrum.*, vol. 77, no. 6, 2006.

[10] P. E. Dewdney, P. J. Hall, R. T. Schilizzi, and T. J. L. W. Lazio, "The square kilometre array," *Proc. IEEE.*, vol. 97, no. 8, pp. 1482–1496, 2009.

[11] S. Schediwy *et al.*, "The mid-frequency square kilometre array phase synchronisation system," *Publ. Astron. Soc. Aust.*, vol. 36, no. e007, 2019.

[12] S. T. Garrington *et al.*, "e-Merlin," *Proc. SPIE.*, vol. 5489, pp. 332–343, 2004.

[13] R. Antil, S. B. Pinki, and S. Beniwal, "An overview of DWDM technology & network," *Int. J. Sci. Technol. Res.*, vol. 1, no. 11, 2012.

[14] M. Rizzi *et al.*, "White rabbit clock characteristics," in *Proc. IEEE Int. Symp. Precis. Clock Synchronization Meas. Control Commun. (ISPCS)*, 2016, pp. 1–6.

[15] T. Wlostowski, "Precise time and frequency transfer in a white rabbit network," Master's thesis, Warsaw Univ. Technol., Warsaw, Poland, May 2011.

[16] G. Daniluk. *White Rabbit Calibration Procedure*. Accessed: Aug. 2020. [Online]. Available: https://www.ohwr.org/documents/213

[17] X. Yuan and B. Wang, "Using single wavelength light to improve the synchronization accuracy of the white rabbit system," *Chin. Opt. Lett.*, vol. 15, no. 10, 2017, Art. no. 101202.

[18] F. Chang, K. Onohara, and T. Mizuochi, "Forward error correction for 100 g transport networks," *IEEE Commun. Mag.*, vol. 48, no. 3, pp. S48–S55, Mar. 2010.

[19] W. Turner, T. Cornwell, A. McPherson, and P. Diamond, "SKA phase 1 system (level 1) requirements specification," *SKA Org. No. SKA-TEL-SKO-0000008 Rev.*, vol. 6, Apr. 2015.

[20] B. Alachkar, A. Wilkinson, and K. Grainge, "Frequency reference stability and coherence loss in radio astronomy interferometers application to the SKA," *J. Astron. Instrum.*, vol. 7, no. 01, 2018, Art. no. 1850001.

[21] I. T. and Union, "Forward error correction for high bit-rate DWDM submarine systems," in *ITU,* Geneva, Switzerland: Tech. Rep. ITU-T G 975, 2013.